

# Modeling Energy Relaxation via Quantum Thermalization: A Superconducting Qubit Coupled to a Many-Body TLS System

Xue-Yi Guo\*

*Beijing Academy of Quantum Information Sciences, Beijing 100193, China*

(Dated: March 17, 2026)

While two-level systems (TLS) in superconducting qubits are known to introduce phonon-mediated energy dissipation channels, many-body TLS systems themselves can also act as a distinct dissipation channel whose effect on qubit energy relaxation remains to be explored. In this work, we model and numerically simulate the irreversible thermalization-driven energy relaxation of a superconducting qubit coupled to a many-body TLS system. Our numerical results show that thermalization suppresses coherent energy exchange between the qubit and TLS, resulting in exponential energy decay. The relaxation times scale as  $T_1, T_2 \propto J^{-2}$ , where  $J$  denotes the qubit-TLS coupling strength. Moreover,  $T_1$  is significantly affected by the internal coupling strength of the TLS system, the TLS frequency fluctuation rate, and the number of thermally excited TLS. This work provides a quantum thermalization perspective for understanding qubit energy relaxation and decoherence, with potential implications for decoherence scenarios in other open quantum systems.

## I. INTRODUCTION

Superconducting qubits, having demonstrated progress in small-scale quantum error correction [1, 2], are regarded as one of the leading candidates for quantum computing research. However, their material environment is complex, rich in microscopic degrees of freedom—both local defects (substrate, interfaces, fabrication residues [3]) and nonlocal excitations (phonons [4], unpaired electrons [5–7]). These microscopic degrees of freedom can couple to superconducting qubits either directly or indirectly, inducing energy relaxation and decoherence, posing a significant obstacle to achieving scalable error correction and practical quantum computation. Understanding these decoherence mechanisms is therefore critical for unlocking the full potential of superconducting quantum processors [3–55].

Local microscopic degrees of freedom can be modeled as two-level systems (TLS) [56–58]. From experiments on superconducting qubits [3, 4, 21, 23, 27, 28, 37, 45] and resonators [9, 10, 12, 13, 18, 19, 30, 32], we know the following about on-chip TLS: (1) TLS are widely present in surface oxide layers [10, 12, 30, 40], superconductor-substrate interfaces [13], residual organic compounds from microfabrication [19], and the bulk of materials [9, 40]; (2) TLS exhibit a broad frequency distribution [26]; (3) The coupling between a superconducting qubit and a TLS is electric-dipole-mediated [28]. Under strong coupling, coherent energy exchange has been observed [21]; (4) Coupling among TLS [18, 21, 22, 26] can induce TLS frequency fluctuations and diffusion, leading to temporal variations in the energy relaxation of superconducting qubits [14, 27, 37]; (5) TLS primarily dissipate energy via phonons [23, 45]; (6) When residing within a phononic band gap, the lifetime of TLS can be significantly prolonged, making them a potential non-

Markovian environment [4].

A common assumption in modeling TLS-induced qubit energy relaxation is that TLS energy dissipates rapidly via phonon channels [11, 42]. For instance, Müller et al. [11] considered a qubit coupled to non-interacting TLS, each possessing its own independent energy dissipation channel. Similarly, the large-scale numerical simulations by Yujin Cho et al. [42], involving nearly one million TLS, assigned a finite relaxation rate to each TLS. The presence of a phonon dissipation channel is essential for suppressing coherent energy exchange between the qubit and TLS—a process that requires continuous error correction [59]. However, engineering the phonon environment can suppress TLS dissipation, enhancing TLS lifetimes [4] and potentially enabling coherent qubit-TLS exchange. In this regime, the impact of interacting many-body TLS systems on superconducting qubit energy relaxation requires further modeling and investigation.

In this work, we model and numerically simulate this chaotic interacting many-body TLS system and demonstrate that thermalization also suppresses qubit-TLS exchange, causing a transition from coherent oscillations to exponential energy relaxation. The resulting qubit energy relaxation time is found to depend on key parameters, including the qubit-TLS coupling strength and the intrinsic properties of the many-body TLS system. The paper is structured as follows. In Sec. II, we introduce the specific model and parameter settings. In Sec. III, we present numerical simulation results under various model parameters, analyzing their influence on the qubit energy relaxation dynamics. Finally, we provide a brief summary and outlook.

## II. MODEL

Our model is shown in Fig. 1(a). The black circle (left) represents the superconducting qubit, and the gold circles (right) represent TLS in the chip materials. Dashed lines indicate their weak resonant electric dipole interaction.

\* guoxy@baqis.ac.cn

Couplings between TLS can be either direct dipole-dipole or phonon-mediated. Experiments [21] have observed strongly interacting TLS pairs via dipole-dipole coupling ( $g = -872\text{MHz}$ ), albeit with low estimated probability. Moreover, experimental evidence [23] suggests that different TLS may couple to the same phonon modes, implying indirect interactions via local phonon modes. We assume near-resonant coupling between TLS with similar frequencies, while disparate-frequency TLS may exhibit ZZ coupling—analogue to cross-Kerr coupling in optics,  $\hat{\sigma}_z^i \hat{\sigma}_z^j$  in spin systems, or  $\hat{n}_i \hat{n}_j$  interactions in lattice models.

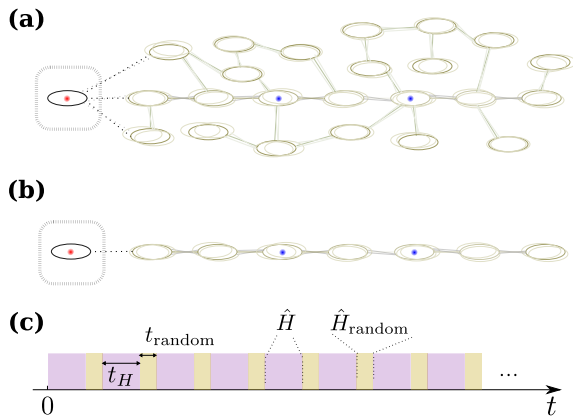


FIG. 1. **Many-Body TLS Model and Full Forward-Time Information Erasure Sequence (FFTIE)**. (a) Coupled superconducting qubit-TLS network. The black circle (dashed box) represents the qubit, and the gold circles represent TLS. Solid lines denote near-resonant TLS-TLS couplings; the dashed line denotes weak near-resonant qubit-TLS coupling. The ghosting effect illustrates TLS with distinct frequencies, with spheres of different colors representing their excited states. (b) One-dimensional chain used for numerical simulations. (c) Full forward-time information erasure sequence (FFTIE) employed in the numerical simulations.

As shown in Refs. [60, 61], a many-body system with two particle types can become chaotic and thermalize rapidly when additional types or an information erasure mechanism is introduced. In our model, TLS with distinct frequencies act as different types, and their frequency fluctuations provide a natural information erasure mechanism.

In numerical simulations, we consider a superconducting qubit coupled to a one-dimensional TLS chain, as illustrated in Fig. (b). A short one-dimensional TLS chain can be viewed as a basic building block of a many-body TLS network. When only two types of TLS,  $\tau$  and  $\nu$ , are considered, the model can be described by a one-dimensional Hubbard model. Its Hamiltonian, denoted

as  $\hat{H}_{\text{TLS}}$ , is given by:

$$\begin{aligned} \hat{H}_{\text{TLS}} = & \sum_{\langle i,j \rangle} \left[ J_{\tau} \left( \hat{c}_{i,\tau}^{\dagger} \hat{c}_{j,\tau} + \hat{c}_{i,\tau} \hat{c}_{j,\tau}^{\dagger} \right) \right. \\ & \left. + J_{\nu} \left( \hat{c}_{i,\nu}^{\dagger} \hat{c}_{j,\nu} + \hat{c}_{i,\nu} \hat{c}_{j,\nu}^{\dagger} \right) \right] \\ & + \sum_i [U_{i,\tau} \hat{n}_{i,\tau} + U_{i,\nu} \hat{n}_{i,\nu}] \\ & + \sum_i U_{\tau,\nu} \hat{n}_{i,\tau} \hat{n}_{i,\nu}. \end{aligned} \quad (1)$$

Assuming the superconducting qubit is resonantly coupled to a  $\tau$ -type TLS at the left end with strength  $J_{q,\tau}$ , the total Hamiltonian of the system is given by:

$$\hat{H} = U_q \hat{n}_q + \hat{H}_{\text{TLS}} + J_{q,\tau} \left( \hat{c}_q^{\dagger} \hat{c}_{0,\tau} + \hat{c}_{0,\tau} \hat{c}_q^{\dagger} \right). \quad (2)$$

To account for random TLS frequency fluctuations, we intersperse time evolution segments governed by the Hamiltonian  $\hat{H}_{\text{random}} = \sum_i U_{i,\nu,\text{random}} \hat{n}_{i,\nu}$  at a certain rate. This results in a sequence that alternates evolution under  $\hat{H}$  and  $\hat{H}_{\text{random}}$ , as illustrated in Fig. 1(c). In contrast to the information erasure sequence  $[\dots \hat{U}^{\dagger}(t_{i+1}) \hat{O}_{i+1} \hat{U}(t_{i+1}) \hat{U}^{\dagger}(t_i) \hat{O}_i \hat{U}(t_i) \dots]$  introduced in Refs. [60, 61], we omit the reverse operations  $\hat{U}^{\dagger}$  to study thermalization dynamics under purely forward-time evolution, and refer to this modified protocol as the full forward-time information erasure sequence (FFTIE). In our implementation, we set  $\hat{U}(t_i) = e^{-i\hat{H}t_H}$  and  $\hat{O}_i = e^{-i\hat{H}_{\text{random}}t_{\text{random}}}$ , with independent random realizations of  $\hat{H}_{\text{random}}$  for each  $\hat{O}_i$ .

### III. NUMERICAL SIMULATION RESULTS

In the total Hamiltonian  $\hat{H}$ , we set  $U_q = 0$  and vary  $J_{q,\tau}$  over the range  $[0.002, 0.1]$ . For the TLS chain, we fix  $J_{\tau} = J_{\nu} = 1$ ,  $U_{i,\tau} = U_{i,\nu} = 0$ , and  $U_{\tau,\nu} = -0.2$ . In  $\hat{H}_{\text{random}}$ , each  $U_{i,\nu,\text{random}}$  is drawn independently from a uniform distribution over  $[0, 3]$ .

When the internal coupling within the TLS chain is strong (much larger than the qubit-TLS coupling  $J_{q,\tau}$ ), the finite chain length results in a discrete energy spectrum. Therefore, the resonance condition between the qubit and the many-body TLS system must be carefully satisfied. For instance, with chain length  $L_{\text{TLS}} = 6$  and  $J_{q,\tau} = 0.01$ , the state  $|1\rangle_q |0\rangle_{\tau} |0\rangle_{\nu}$  is approximately an energy eigenstate of  $\hat{H}$ . Consequently, the qubit occupation  $\langle \hat{n}_q \rangle$  remains nearly constant, as shown by the blue curve in Fig. 2. For  $L_{\text{TLS}} = 7$ , however, this state forms a superposition of coupled-system energy eigenstates, leading to complete coherent energy exchange between the qubit and the one-dimensional chain, as illustrated by the orange curve in Fig. 2. If the internal TLS chain coupling is comparable to  $J_{q,\tau}$ , the qubit energy propagates through the chain analogously to a single-photon quantum walk. In this regime, the chain length has little effect on the

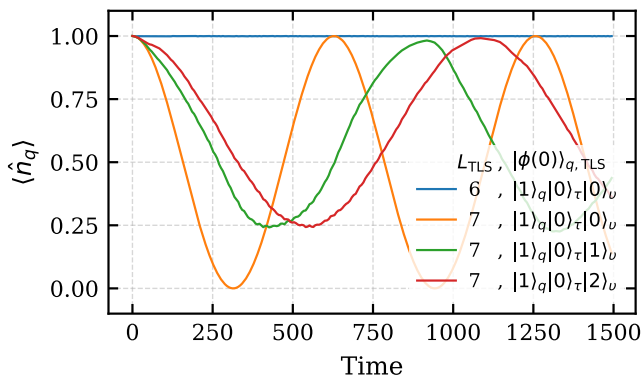


FIG. 2. **Coherent Qubit-TLS Chain Energy Exchange.** Time evolution of the qubit occupation  $\langle \hat{n}_q \rangle$  for many-body TLS chain lengths  $L_{\text{TLS}} = 6$  and  $7$ , starting from different initial states  $|\phi(0)\rangle_{q,\text{TLS}}$ .

amplitude of coherent energy exchange. To effectively simulate a continuous-spectrum environment across different parameter regimes, we choose a TLS chain length of  $L_{\text{TLS}} = 7$ .

The number of TLS excitations also affects the coherent energy exchange. For a single  $\nu$ -type excitation, i.e., the initial state  $|0000000\rangle_\tau|1000000\rangle_\nu$  (denoted succinctly as  $|0\rangle_\tau|1\rangle_\nu$ ), the qubit exhibits the coherent oscillation shown by the green curve in Fig. 2, with an increased period and decreased amplitude. When the  $\nu$ -type excitation number is increased to two, the period further increases while the amplitude remains almost unchanged. Since TLS excitation probabilities are low under typical low-temperature experimental conditions, we focus primarily on few-excitation regimes.

Such coherent energy exchange between the qubit and TLS in superconducting quantum chips demands high error-correction rates (continuous quantum error correction) [59], which is challenging to achieve experimentally. In contrast, we demonstrate that many-body TLS thermalization suppresses this coherent qubit-TLS exchange, transforming it into exponential energy relaxation—a feature beneficial for practical quantum error correction. As shown in Fig. 3, starting from  $|\phi(0)\rangle_{q,\text{TLS}} = |1\rangle_q|0\rangle_\tau|2\rangle_\nu$ , the combined system evolves unitarily under the FFTIE sequence and remains in the pure state  $|\phi(t)\rangle_{q,\text{TLS}}$ . With  $J_{q,\tau} = 0.01$ ,  $t_H = 2$ , and  $t_{\text{random}} = 0.5$ , the qubit occupation  $\langle \hat{n}_q \rangle$  exhibits exponential decay across individual trajectories (Fig. 3(a), thin lines), each displaying consistent decay profiles—signifying irreversible thermalization.

The solid blue line in Fig. 3(a) represents the average  $\langle \langle \hat{n}_q \rangle \rangle_{\text{random}}$  over 10 individual evolutions, where  $\langle \cdot \rangle_{\text{random}}$  denotes averaging over different energy relaxation trajectories. Due to the random parameters in  $\hat{H}_{\text{TLS},\text{random}}$  within the sequence, each individual evolution  $|\phi(t)\rangle_{q,\text{TLS}}$  exhibits small stochastic fluctuations. The averaged exponential decay curve becomes significantly smoother and eventually saturates to an equi-

librium value of  $1/8$ . The light blue shaded region in Fig. 3(a) covers one standard deviation above and below the mean. It is worth noting that in experiments, obtaining the probability of the qubit being in  $|1\rangle_q$  at time  $t$  requires repeated state preparation, evolution, and measurement—a procedure that inherently includes averaging over random energy relaxation processes. Consequently, the experimentally measured  $T_1$  curve corresponds to this averaged result, analogous to the solid blue line in Fig. 3(a).

Under the same FFTIE sequence, the relaxation dynamics of  $\sqrt{\langle \hat{\sigma}_x \rangle^2 + \langle \hat{\sigma}_y \rangle^2}$  are shown in Fig. 3(b) for the qubit initialized in  $(|0\rangle + |1\rangle)/\sqrt{2}$ . The thin light lines (10 trajectories) each exhibit a clear irreversible thermalization process. The solid orange line represents the average  $\langle \sqrt{\langle \hat{\sigma}_x \rangle^2 + \langle \hat{\sigma}_y \rangle^2} \rangle_{\text{random}}$  over the 10 trajectories, displaying a pronounced exponential decay trend.

Figures 3(d) and (e) present the numerical results of  $\langle \langle \hat{n}_q \rangle \rangle_{\text{random}}$  and  $\langle \sqrt{\langle \hat{\sigma}_x \rangle^2 + \langle \hat{\sigma}_y \rangle^2} \rangle_{\text{random}}$  (dashed lines) for  $J_{q,\tau} = 0.01, 0.008, 0.006, 0.004, 0.002$ , with the corresponding exponential fits shown as solid lines. In Fig. 3(f), the extracted  $T_1$  values (blue open squares) are  $6131.4(\pm 56.8)$ ,  $9430.9(\pm 73.1)$ ,  $17764.3(\pm 127.3)$ ,  $36730.1(\pm 145.1)$ , and  $154159.9(\pm 493.1)$ ; the extracted  $T_2$  values (orange open squares) are  $12484.8(\pm 57.2)$ ,  $23615.2(\pm 155.5)$ ,  $37487.0(\pm 407.2)$ ,  $68364.3(\pm 704.4)$ , and  $337756.4(\pm 16337.9)$ . Error bars represent fitting uncertainties, and the dashed lines are power-law fits to the data. The fitted  $T_1$  values scale as  $J_{q,\tau}^{-1.9969}$ , while  $T_2$  scales as  $J_{q,\tau}^{-1.9676}$ . Moreover, the fitting results show that  $T_2$  is approximately 2.14 times  $T_1$ . In our model, the qubit is only weakly coupled to the TLS chain without additional noise sources; consequently, its dephasing arises solely from energy relaxation. Setting  $J_{q,\tau}$  in MHz and recalling  $\hbar = 1$ , the extracted  $T_1$  values convert to  $975.88(\pm 9.04)$ ,  $1501.01(\pm 11.64)$ ,  $2827.45(\pm 20.26)$ ,  $5846.01(\pm 23.10)$ , and  $24536.80(\pm 78.49)$   $\mu\text{s}$ . The smallest of these is comparable to experimental values [47], serving as a useful reference.

When  $J_{q,\tau}$  is further increased, the qubit energy relaxation gradually transitions from exponential decay to oscillatory decay. Figure 3(c) shows the numerical results for  $J_{q,\tau} = 0.1$ . Both individual trajectories and the average exhibit clear oscillatory decay behavior, consistent with the relaxation features observed experimentally in the strong qubit-TLS coupling regime[21]. The fitted  $T_1$  value is  $81.7(\pm 1.2)$ , which is close to the extrapolated value of  $61.8$  obtained from Fig. 3(f).

The simulated  $T_1$  scaling with  $J_{q,\tau}$  indicates that  $T_1$  is primarily governed by  $J_{q,\tau}$  under fixed environmental conditions. In practice, however, TLS system parameters—such as internal couplings, frequency fluctuations, and thermal excitation numbers—vary across chips due to fabrication and experimental conditions [14]. From the Lindblad master equation perspective, such variations modify environmental correlation functions and thus the qubit energy relaxation rate. We now numerically explore this dependence by simulating qubit

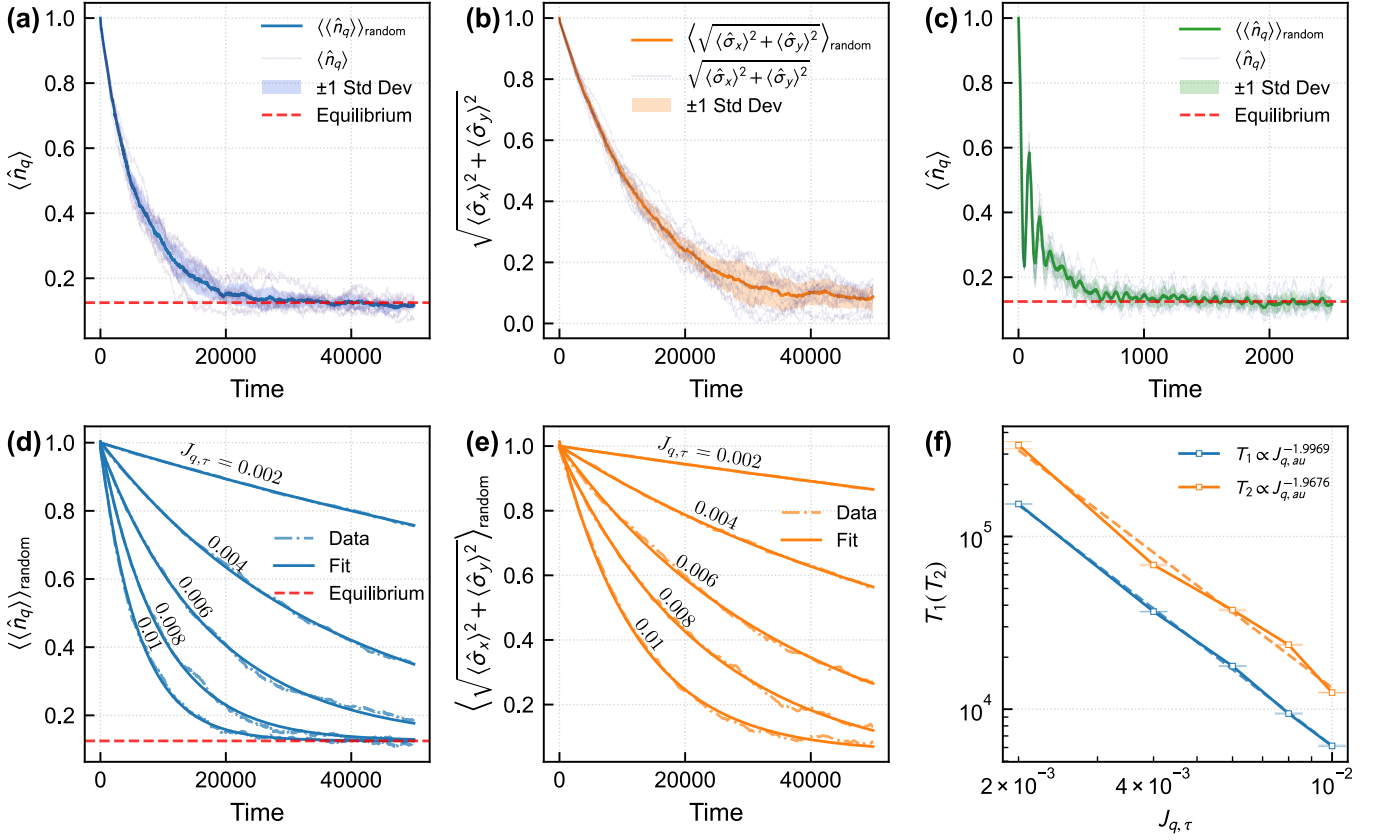


FIG. 3. **Exponential Energy Relaxation and Dephasing Induced by Thermalization.** (a) and (b) Time evolution of the qubit's occupation  $\langle \hat{n}_q \rangle$  and coherence  $\sqrt{\langle \hat{\sigma}_x \rangle^2 + \langle \hat{\sigma}_y \rangle^2}$  for  $J_{q,\tau} = 0.01$ , with initial states  $|1\rangle$  and  $(|0\rangle + |1\rangle)/\sqrt{2}$ , respectively. Solid blue (orange) lines represent averages over 10 trajectories, shaded regions indicate standard deviations, and thin light lines show individual trajectories. (c) Time evolution of  $\langle \hat{n}_q \rangle$  for  $J_{q,\tau} = 0.1$  (initial state  $|1\rangle$ ). The solid green line represents the average over 10 trajectories, the shaded region indicates the standard deviation, and the thin light lines show individual trajectories. (d) and (e) Time evolution of  $\langle \hat{n}_q \rangle_{\text{random}}$  and  $\sqrt{\langle \hat{\sigma}_x \rangle^2 + \langle \hat{\sigma}_y \rangle^2}_{\text{random}}$  for  $J_{q,\tau} = 0.01, 0.008, 0.006, 0.004, 0.002$ , with initial states  $|1\rangle$  and  $(|0\rangle + |1\rangle)/\sqrt{2}$ , respectively. Solid lines are exponential fits, and dashed lines represent the averaged raw data (each average containing 10 trajectories). (f) Extracted  $T_1$  and  $T_2$  values as functions of  $J_{q,\tau}$ . The dashed lines are fits to the data, with error bars derived from the fitting uncertainties of  $T_1$  and  $T_2$  in panels (d) and (e).

relaxation under different many-body TLS parameters.

Figure 4(a) shows the qubit energy relaxation curves for  $J_\tau$  and  $J_\nu$  set to 0.2, 0.5, 1, 3, and 7, respectively, with all other parameters identical to those in Fig. 3(a). It is observed that for  $J_\tau$  and  $J_\nu > 3$ , the qubit energy relaxation time reaches a maximum and remains constant. As  $J_\tau$  and  $J_\nu$  decrease,  $T_1$  becomes shorter and exhibits increased sensitivity in the regime below 1. These results indicate that, under otherwise fixed conditions, stronger internal TLS coupling can enhance the qubit lifetime.

The parameter  $t_H$  in the FFTIE sequence plays a crucial role in the qubit energy relaxation dynamics and is associated with the TLS frequency fluctuation rate. Figure 4(b) shows the qubit energy relaxation curves for  $t_H = \infty, 90, 50, 10, 6, 2$ , and 1. All other parameters are the same as in Fig. 3(a). For  $t_H = \infty$ , the system exhibits coherent energy exchange between the qubit and the TLS chain, with an oscillation period of approximately 1093. Notably, even at its minima, the qubit energy remains

significantly above the thermal equilibrium value. When the  $e^{-i\hat{H}_{\text{random}}t_{\text{random}}}$  is inserted with a relatively low rate, e.g.,  $t_H = 90$ , the coherent exchange remains discernible for up to three oscillation cycles before rapidly decaying to thermal equilibrium. At  $t_H = 50$ , coherent exchange is completely suppressed. As  $t_H$  decreases further, the decay curves diverge from the coherent exchange curve from the very beginning (see inset in Fig. 4(b)) and exhibit clear exponential decay at long times. Thus, increasing the FFTIE rate suppresses coherent oscillations and prolongs qubit lifetime—benefiting quantum error correction.

Figure 4(c) uses the same parameters as Fig. 3(d), except that the number of  $\nu$ -type TLS excitations is reduced from 2 to 1. The resulting qubit energy relaxation curves for different  $J_{q,\tau}$  yield fitted  $T_1$  values of  $2886.9(\pm 114.5)$ ,  $4489.7(\pm 94.8)$ ,  $6709.7(\pm 169.2)$ ,  $16574.1(\pm 198.5)$ , and  $65361.3(\pm 257.9)$ . The extracted scaling  $T_1 \propto J_{q,\tau}^{-1.944}$  is consistent with Fig. 3(d). How-

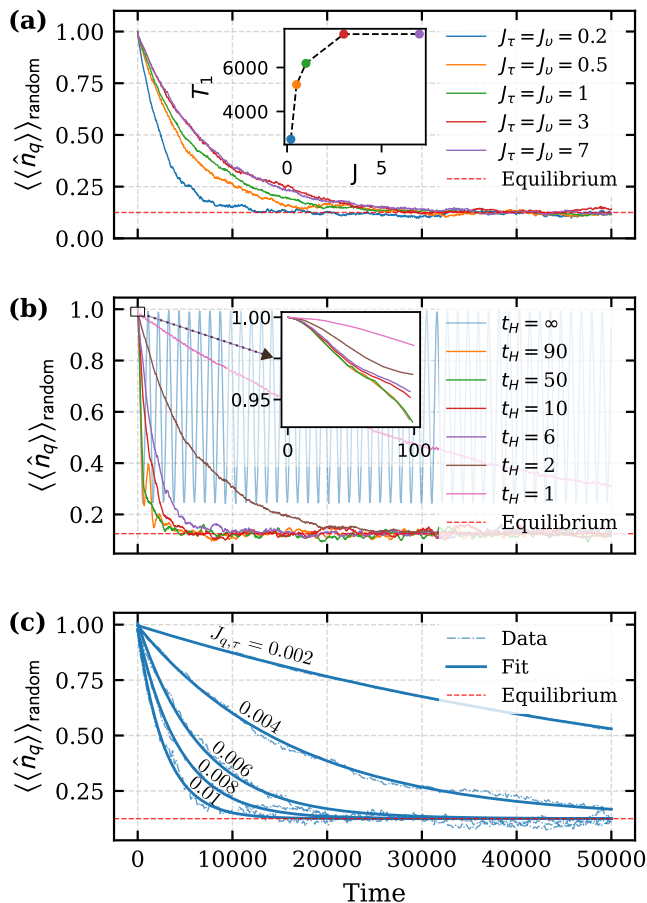


FIG. 4. **Qubit Energy Relaxation Under Different Many-Body TLS Parameters.** (a) Average  $T_1$  over 5 trajectories for varying  $J_\tau, J_\nu$ . Other parameters as in Fig. 3(a). (b) Average  $T_1$  over 5 trajectories for different  $t_H$ . Other parameters as in Fig. 3(a). (c) Average  $T_1$  over 5 trajectories (dashed) with exponential fits (solid). Parameters as in Fig. 3(d), but with initial TLS state  $|0\rangle_\tau|1\rangle_\nu$  (single  $\nu$ -excitation).

ever, the  $T_1$  values are reduced by nearly half compared to those in Fig. 3(d). In experiments, TLS excitation probabilities are temperature-dependent. Our simulations indicate that, under certain conditions, fewer excited TLS (i.e., lower temperatures) can actually shorten the qubit lifetime.

#### IV. SUMMARY AND OUTLOOK

TLS on superconducting quantum chips induce two distinct dissipation channels: the first is the phonon dissipation channel mediated by TLS, and the second is the many-body TLS system itself. The former has been widely studied and is considered the dominant dissipation channel. However, when the coupling between TLS and nonlocal phonon degrees of freedom is suppressed, TLS lifetimes can be significantly enhanced [4], rendering the dissipation channel arising from the many-body TLS system non-negligible. In this work, we model and analyze the energy relaxation dynamics under this specific regime.

When a superconducting qubit couples to a single TLS, coherent energy exchange emerges, necessitating continuous error correction [59]. Our results show that the chaotic and thermalizing nature of many-body TLS systems suppresses such oscillations. By prolonging thermalization time, this mechanism enhances qubit coherence—a feature beneficial for quantum error correction.

The information erasure theory developed in Refs. [60, 61] reveals general principles of quantum chaos and irreversible thermalization, offering a framework for analyzing such processes. Using this approach, we simulate the thermalization dynamics of a qubit coupled to a one-dimensional many-body TLS chain. In our model, stronger internal TLS coupling, higher FFTIE rates (i.e., TLS fluctuation rates), and more excited TLS all suppress coherent oscillations more effectively, extending qubit lifetime. Furthermore, the qubit relaxation time scales as  $J_{q,\tau}^{-2}$ , indicating that weaker qubit-TLS coupling is preferable. The simulated relaxation dynamics depend on multiple parameters, offering insight into the experimental instability of  $T_1$  [26, 47]—a phenomenon that also poses challenges for quantum error correction [62–64].

In future experiments, advanced TLS control techniques [3, 21, 27, 28, 49] can be employed to probe their effect on qubit relaxation. One may also tune the number of excited TLS [4] and observe the corresponding changes in qubit relaxation dynamics. Theoretically, the one-dimensional TLS chain studied here is a simplified model; realistic devices likely host networks of such coupled chains. Future work could explore larger-scale simulations of these networks.

[1] R. Acharya, D. A. Abanin, L. Aghababaie-Beni, I. Aleiner, T. I. Andersen, M. Ansmann, F. Arute, K. Arya, A. Asfaw, N. Astrakhantsev, J. Atalaya, R. Babbush, D. Bacon, B. Ballard, J. C. Bardin, J. Bausch, A. Bengtsson, A. Bilmes, S. Blackwell, S. Boixo, G. Bortoli, A. Bourassa, J. Bovaird, L. Brill, M. Broughton, D. A. Browne, B. Buchea, B. B. Buckley, D. A. Buell, T. Burger, B. Burkett, N. Bushnell, A. Cabrera, J. Campero, H.-S. Chang, Y. Chen, Z. Chen,

B. Chiaro, D. Chik, C. Chou, J. Claes, A. Y. Cleland, J. Cogan, R. Collins, P. Conner, W. Courtney, A. L. Crook, B. Curtin, S. Das, A. Davies, L. De Lorenzo, D. M. Debroy, S. Demura, M. Devoret, A. Di Paolo, P. Donohoe, I. Drozdov, A. Dunsworth, C. Earle, T. Edlich, A. Eickbusch, A. M. Elbag, M. Elzouka, C. Erickson, L. Faoro, E. Farhi, V. S. Ferreira, L. F. Burgos, E. Forati, A. G. Fowler, B. Foxen, S. Ganjam, G. Garcia, R. Gasca, . Genois, W. Giang, C. Gid-

- ney, D. Gilboa, R. Gosula, A. G. Dau, D. Graumann, A. Greene, J. A. Gross, S. Habegger, J. Hall, M. C. Hamilton, M. Hansen, M. P. Harrigan, S. D. Harrington, F. J. H. Heras, S. Heslin, P. Heu, O. Higgott, G. Hill, J. Hilton, G. Holland, S. Hong, H.-Y. Huang, A. Huff, W. J. Huggins, L. B. Ioffe, S. V. Isakov, J. Iveland, E. Jeffrey, Z. Jiang, C. Jones, S. Jordan, C. Joshi, P. Juhas, D. Kafri, H. Kang, A. H. Karamlou, K. Kechedzhi, J. Kelly, T. Khairi, T. Khattar, M. Khezri, S. Kim, P. V. Klimov, A. R. Klots, B. Kobrin, P. Kohli, A. N. Korotkov, F. Kostritsa, R. Kothari, B. Kozlovskii, J. M. Kreikebaum, V. D. Kurilovich, N. Lacroix, D. Landhuis, T. Lange-Dei, B. W. Langley, P. Laptev, K.-M. Lau, L. Le Guevel, J. Ledford, J. Lee, K. Lee, Y. D. Lensky, S. Leon, B. J. Lester, W. Y. Li, Y. Li, A. T. Lill, W. Liu, W. P. Livingston, A. Locharla, E. Lucero, D. Lundahl, A. Lunt, S. Madhuk, F. D. Malone, A. Maloney, S. Mandrà, J. Manyika, L. S. Martin, O. Martin, S. Martin, C. Maxfield, J. R. McClean, M. McEwen, S. Meeks, A. Megrant, X. Mi, K. C. Miao, A. Mieszala, R. Molavi, S. Molina, S. Montazeri, A. Morvan, R. Movassagh, W. Mruczkiewicz, O. Naaman, M. Neeley, C. Neill, A. Nersisyan, H. Neven, M. Newman, J. H. Ng, A. Nguyen, M. Nguyen, C.-H. Ni, M. Y. Niu, T. E. O'Brien, W. D. Oliver, A. Opremcak, K. Ottosson, A. Petukhov, A. Pizzuto, J. Platt, R. Potter, O. Pritchard, L. P. Pryadko, C. Quintana, G. Ramachandran, M. J. Reagor, J. Redding, D. M. Rhodes, G. Roberts, E. Rosenberg, E. Rosenfeld, P. Roushan, N. C. Rubin, N. Saei, D. Sank, K. Sankaragomathi, K. J. Satzinger, H. F. Schurkus, C. Schuster, A. W. Senior, M. J. Shearn, A. Shorter, N. Shutty, V. Shvarts, S. Singh, V. Sivak, J. Skrzynny, S. Small, V. Smelyanskiy, W. C. Smith, R. D. Somma, S. Springer, G. Sterling, D. Strain, J. Suchard, A. Szasz, A. Szein, D. Thor, A. Torres, M. M. Torunbalci, A. Vaishnav, J. Vargas, S. Vdovichev, G. Vidal, B. Villalonga, C. V. Heidweiller, S. Waltman, S. X. Wang, B. Ware, K. Weber, T. Weidel, T. White, K. Wong, B. W. K. Woo, C. Xing, Z. J. Yao, P. Yeh, B. Ying, J. Yoo, N. Yosri, G. Young, A. Zalcman, Y. Zhang, N. Zhu, N. Zobrist, and Google Quantum AI and Collaborators, Quantum error correction below the surface code threshold, *Nature* **638**, 920 (2025).
- [2] T. He, W. Lin, R. Wang, Y. Li, J. Bei, J. Cai, S. Cao, D. Chen, K. Chen, X. Chen, Z. Chen, Z. Chen, Z. Chen, W. Chu, H. Deng, X. Ding, Z. Ding, B. Fan, D. Fan, Y. Fu, D. Gao, M. Gong, J. Gui, C. Guo, S. Guo, L. Han, L. Hong, Y. Hu, H.-L. Huang, Y.-H. Huo, C. Jiang, L. Jiang, T. Jiang, Z. Jiang, H. Jin, D. Li, D. Li, J. Li, J. Li, J. Li, J. Li, N. Li, S. Li, Y. Li, F. Liang, N. Liao, J. Lin, K. Liu, M. Liu, Y. Liu, H. Lou, Y. Ma, K. Nan, M. Nie, L. Niu, W. Peng, H. Qian, H. Rong, T. Rong, H. Shen, Q. Shen, H. Su, F. Su, C. Sun, L. Sun, T. Sun, Y. Sun, Y. Tan, J. Tan, W. Tu, J. Wang, B. Wang, C. Wang, C. Wang, C. Wang, J. Wang, S. Wang, X. Wang, Z. Wei, D. Wu, G. Wu, Y. Wu, Y. Xu, C. Xue, K. Yan, X. Yan, W. Yang, X. Yang, Y. Yang, Y. Ye, Z. Ye, Z. Yi, C. Ying, J. Yu, Q. Yu, X. Zeng, C. Zha, S. Zhan, H. Zhang, H. Zhang, K. Zhang, W. Zhang, Y. Zhang, Y. Zhang, Z. Zhang, G. Zhao, X. Zhao, Y. Zhao, Z. Zhao, L. Zheng, F. Zhou, L. Zhou, N. Zhou, N. Zhou, C. Zhu, Q. Zhu, G. Zou, H. Zou, Q. Zhang, C.-Y. Lu, C.-Z. Peng, F. Chen, X. Zhu, and J.-W. Pan, Experimental Quantum Error Correction below the Surface Code Threshold via All-Microwave Leakage Suppression, *Physical Review Letters* **135**, 260601 (2025).
- [3] A. Bilmes, A. Megrant, P. Klimov, G. Weiss, J. M. Martinis, A. V. Ustinov, and J. Lisenfeld, Resolving the positions of defects in superconducting quantum bits, *Scientific Reports* **10**, 3090 (2020).
- [4] M. Odeh, K. Godeneli, E. Li, R. Tangirala, H. Zhou, X. Zhang, Z.-H. Zhang, and A. Sipahigil, Non-Markovian dynamics of a superconducting qubit in a phononic bandgap, *Nature Physics* **21**, 406 (2025).
- [5] R. Barends, J. Wenner, M. Lenander, Y. Chen, R. C. Bialczak, J. Kelly, E. Lucero, P. O'Malley, M. Mariantoni, D. Sank, H. Wang, T. C. White, Y. Yin, J. Zhao, A. N. Cleland, J. M. Martinis, and J. J. A. Baselmans, Minimizing quasiparticle generation from stray infrared light in superconducting quantum circuits, *Applied Physics Letters* **99**, 113507 (2011).
- [6] S. Gustavsson, F. Yan, G. Catelani, J. Bylander, A. Kamal, J. Birenbaum, D. Hover, D. Rosenberg, G. Samach, A. P. Sears, S. J. Weber, J. L. Yoder, J. Clarke, A. J. Kerman, F. Yoshihara, Y. Nakamura, T. P. Orlando, and W. D. Oliver, Suppressing relaxation in superconducting qubits by quasiparticle pumping, *Science* , aah5844 (2016).
- [7] S. E. d. Graaf, L. Faoro, L. B. Ioffe, S. Mahashabde, J. J. Burnett, T. Lindström, S. E. Kubatkin, A. V. Danilov, and A. Y. Tzalenchuk, Two-level systems in superconducting quantum devices due to trapped quasiparticles, *Science Advances* **10**, 1126/sciadv.abc5055 (2020).
- [8] L.-C. Ku and C. C. Yu, Decoherence of a Josephson qubit due to coupling to two-level systems, *Physical Review B* **72**, 024526 (2005).
- [9] A. D. O'Connell, M. Ansmann, R. C. Bialczak, M. Hofheinz, N. Katz, E. Lucero, C. McKenney, M. Neeley, H. Wang, E. M. Weig, A. N. Cleland, and J. M. Martinis, Microwave dielectric loss at single photon energies and millikelvin temperatures, *Applied Physics Letters* **92**, 112903 (2008).
- [10] J. Gao, M. Daal, A. Vayonakis, S. Kumar, J. Zmuidzinas, B. Sadoulet, B. A. Mazin, P. K. Day, and H. G. Leduc, Experimental evidence for a surface distribution of two-level systems in superconducting lithographed microwave resonators, *Applied Physics Letters* **92**, 152505 (2008).
- [11] C. Müller, A. Shnirman, and Y. Makhlin, Relaxation of Josephson qubits due to strong coupling to two-level systems, *Physical Review B* **80**, 134517 (2009).
- [12] H. Wang, M. Hofheinz, J. Wenner, M. Ansmann, R. C. Bialczak, M. Lenander, E. Lucero, M. Neeley, A. D. O'Connell, D. Sank, M. Weides, A. N. Cleland, and J. M. Martinis, Improving the coherence time of superconducting coplanar resonators, *Applied Physics Letters* **95**, 233508 (2009).
- [13] D. S. Wisbey, J. Gao, M. R. Vissers, F. C. S. da Silva, J. S. Kline, L. Vale, and D. P. Pappas, Effect of metal/substrate interfaces on radio-frequency loss in superconducting coplanar waveguides, *Journal of Applied Physics* **108**, 093918 (2010).
- [14] Y. Shalibo, Y. Rofer, D. Shwa, F. Zeides, M. Neeley, J. M. Martinis, and N. Katz, Lifetime and Coherence of Two-Level Defects in a Josephson Junction, *Physical Review Letters* **105**, 177001 (2010).
- [15] M. S. Khalil, F. C. Wellstood, and K. D. Osborn, Loss Dependence on Geometry and Applied Power in Super-

- conducting Coplanar Resonators, *IEEE Transactions on Applied Superconductivity* **21**, 879 (2011).
- [16] J. M. Sage, V. Bolkhovskiy, W. D. Oliver, B. Turek, and P. B. Welander, Study of loss in superconducting coplanar waveguide resonators, *Journal of Applied Physics* **109**, 063915 (2011).
- [17] A. Megrant, C. Neill, R. Barends, B. Chiaro, Y. Chen, L. Feigl, J. Kelly, E. Lucero, M. Mariantoni, P. J. J. O'Malley, D. Sank, A. Vainsencher, J. Wenner, T. C. White, Y. Yin, J. Zhao, C. J. Palmstrom, J. M. Martinis, and A. N. Cleland, Planar superconducting resonators with internal quality factors above one million, *Applied Physics Letters* **100**, 113510 (2012).
- [18] J. Burnett, L. Faoro, I. Wisby, V. L. Gurtovoi, A. V. Chernykh, G. M. Mikhailov, V. A. Tulin, R. Shaikhaidarov, V. Antonov, P. J. Meeson, A. Y. Tzalenchuk, and T. Lindström, Evidence for interacting two-level systems from the  $1/f$  noise of a superconducting resonator, *Nature Communications* **5**, 4119 (2014).
- [19] C. M. Quintana, A. Megrant, Z. Chen, A. Dunsworth, B. Chiaro, R. Barends, B. Campbell, Y. Chen, I.-C. Hoi, E. Jeffrey, J. Kelly, J. Y. Mutus, P. J. J. O'Malley, C. Neill, P. Roushan, D. Sank, A. Vainsencher, J. Wenner, T. C. White, A. N. Cleland, and J. M. Martinis, Characterization and reduction of microfabrication-induced decoherence in superconducting quantum circuits, *Applied Physics Letters* **105**, 062601 (2014).
- [20] L. Faoro and L. B. Ioffe, Interacting tunneling model for two-level systems in amorphous materials and its predictions for their dephasing and noise in superconducting microresonators, *Physical Review B* **91**, 014201 (2015).
- [21] J. Lisenfeld, G. J. Grabovskij, C. Müller, J. H. Cole, G. Weiss, and A. V. Ustinov, Observation of directly interacting coherent two-level systems in an amorphous material, *Nature Communications* **6**, 6182 (2015).
- [22] C. Müller, J. Lisenfeld, A. Shnirman, and S. Poletto, Interacting two-level defects as sources of fluctuating high-frequency noise in superconducting circuits, *Physical Review B* **92**, 035442 (2015).
- [23] J. Lisenfeld, A. Bilmes, S. Matityahu, S. Zanker, M. Marthaler, M. Schechter, G. Schön, A. Shnirman, G. Weiss, and A. V. Ustinov, Decoherence spectroscopy with individual two-level tunneling defects, *Scientific Reports* **6**, 23786 (2016).
- [24] S. Matityahu, A. Shnirman, G. Schön, and M. Schechter, Decoherence of a quantum two-level system by spectral diffusion, *Physical Review B* **93**, 134208 (2016).
- [25] N. Kirsh, E. Svetitsky, A. L. Burin, M. Schechter, and N. Katz, Revealing the nonlinear response of a tunneling two-level system ensemble using coupled modes, *Physical Review Materials* **1**, 012601 (2017).
- [26] P. Klimov, J. Kelly, Z. Chen, M. Neeley, A. Megrant, B. Burkett, R. Barends, K. Arya, B. Chiaro, Y. Chen, A. Dunsworth, A. Fowler, B. Foxen, C. Gidney, M. Giustina, R. Graff, T. Huang, E. Jeffrey, E. Lucero, J. Mutus, O. Naaman, C. Neill, C. Quintana, P. Roushan, D. Sank, A. Vainsencher, J. Wenner, T. White, S. Boixo, R. Babbush, V. Smelyanskiy, H. Neven, and J. Martinis, Fluctuations of Energy-Relaxation Times in Superconducting Qubits, *Physical Review Letters* **121**, 090502 (2018).
- [27] S. M. Meißner, A. Seiler, J. Lisenfeld, A. V. Ustinov, and G. Weiss, Probing individual tunneling fluctuators with coherently controlled tunneling systems, *Physical Review B* **97**, 180505 (2018).
- [28] J. Lisenfeld, A. Bilmes, A. Megrant, R. Barends, J. Kelly, P. Klimov, G. Weiss, J. M. Martinis, and A. V. Ustinov, Electric field spectroscopy of material defects in transmon qubits, *npj Quantum Information* **5**, 1 (2019).
- [29] S. Schlör, J. Lisenfeld, C. Müller, A. Bilmes, A. Schneider, D. P. Pappas, A. V. Ustinov, and M. Weides, Correlating Decoherence in Transmon Qubits: Low Frequency Noise by Single Fluctuators, *Physical Review Letters* **123**, 190502 (2019).
- [30] W. Woods, G. Calusine, A. Melville, A. Sevi, E. Golden, D. Kim, D. Rosenberg, J. Yoder, and W. Oliver, Determining Interface Dielectric Losses in Superconducting Coplanar-Waveguide Resonators, *Physical Review Applied* **12**, 014012 (2019).
- [31] T. Capelle, E. Flurin, E. Ivanov, J. Palomo, M. Rosticher, S. Chua, T. Briant, P.-F. Cohadon, A. Heidmann, T. Jacqmin, and S. Deléglise, Probing a Two-Level System Bath via the Frequency Shift of an Off-Resonantly Driven Cavity, *Physical Review Applied* **13**, 034022 (2020).
- [32] C. R. H. McRae, H. Wang, J. Gao, M. R. Vissers, T. Brecht, A. Dunsworth, D. P. Pappas, and J. Mutus, Materials loss measurements using superconducting microwave resonators, *Review of Scientific Instruments* **91**, 091101 (2020).
- [33] A. P. M. Place, L. V. H. Rodgers, P. Mundada, B. M. Smitham, M. Fitzpatrick, Z. Leng, A. Premkumar, J. Bryon, A. Vrajitoarea, S. Sussman, G. Cheng, T. Madhavan, H. K. Babla, X. H. Le, Y. Gang, B. Jäck, A. Geynis, N. Yao, R. J. Cava, N. P. de Leon, and A. A. Houck, New material platform for superconducting transmon qubits with coherence times exceeding 0.3 milliseconds, *Nature Communications* **12**, 1779 (2021).
- [34] X. You, A. A. Clerk, and J. Koch, Positive- and negative-frequency noise from an ensemble of two-level fluctuators, *Physical Review Research* **3**, 013045 (2021).
- [35] S. E. de Graaf, S. Mahashabde, S. E. Kubatkin, A. Y. Tzalenchuk, and A. V. Danilov, Quantifying dynamics and interactions of individual spurious low-energy fluctuators in superconducting circuits, *Physical Review B* **103**, 174103 (2021).
- [36] G. Andersson, A. L. O. Bilobran, M. Scigliuzzo, M. M. de Lima, J. H. Cole, and P. Delsing, Acoustic spectral hole-burning in a two-level system ensemble, *npj Quantum Information* **7**, 15 (2021).
- [37] M. Carroll, S. Rosenblatt, P. Jurcevic, I. Lauer, and A. Kandala, Dynamics of superconducting qubit relaxation times, *npj Quantum Information* **8**, 132 (2022).
- [38] C.-C. Hung, Probing Hundreds of Individual Quantum Defects in Polycrystalline and Amorphous Alumina, *Physical Review Applied* **17**, 10.1103/PhysRevApplied.17.034025 (2022).
- [39] X. You, Z. Huang, U. Alyanak, A. Romanenko, A. Grassellino, and S. Zhu, Stabilizing and Improving Qubit Coherence by Engineering the Noise Spectrum of Two-Level Systems, *Physical Review Applied* **18**, 044026 (2022).
- [40] K. D. Crowley, R. A. McLellan, A. Dutta, N. Shumiya, A. P. Place, X. H. Le, Y. Gang, T. Madhavan, M. P. Bland, R. Chang, N. Khedkar, Y. C. Feng, E. A. Umbarkar, X. Gui, L. V. Rodgers, Y. Jia, M. M. Feldman, S. A. Lyon, M. Liu, R. J. Cava, A. A. Houck, and N. P. de Leon, Disentangling Losses in Tantalum Superconducting Circuits, *Physical Review X* **13**, 041005 (2023).

- [41] M. Lucas, A. V. Danilov, L. V. Levitin, A. Jayaraman, A. J. Casey, L. Faoro, A. Y. Tzalenchuk, S. E. Kubatkin, J. Saunders, and S. E. de Graaf, Quantum bath suppression in a superconducting circuit by immersion cooling, *Nature Communications* **14**, 3522 (2023).
- [42] Y. Cho, D. Jasrasaria, K. G. Ray, D. M. Tennant, V. Lordi, J. L. DuBois, and Y. J. Rosen, Simulating noise on a quantum processor: interactions between a qubit and resonant two-level system bath, *Quantum Science and Technology* **8**, 045023 (2023).
- [43] T. Thorbeck, A. Eddins, I. Lauer, D. T. McClure, and M. Carroll, Two-Level-System Dynamics in a Superconducting Qubit Due to Background Ionizing Radiation, *PRX Quantum* **4**, 020356 (2023).
- [44] M. Spiecker, P. Paluch, N. Gosling, N. Drucker, S. Matityahu, D. Gusenkova, S. Günzler, D. Rieger, I. Takmakov, F. Valenti, P. Winkel, R. Gebauer, O. Sander, G. Catelani, A. Shnirman, A. V. Ustinov, W. Wernsdorfer, Y. Cohen, and I. M. Pop, Two-level system hyperpolarization using a quantum Szilard engine, *Nature Physics* **19**, 1320 (2023).
- [45] M. Chen, J. C. Owens, H. Putterman, M. Schäfer, and O. Painter, Phonon engineering of atomic-scale defects in superconducting quantum circuits, *Science Advances* **10**, eado6240 (2024).
- [46] M. Spiecker, A. I. Pavlov, A. Shnirman, and I. M. Pop, Solomon equations for qubit and two-level systems: Insights into non-Poissonian quantum jumps, *Physical Review A* **109**, 052218 (2024).
- [47] M. P. Bland, F. Bahrami, J. G. C. Martinez, P. H. Presteggaard, B. M. Smitham, A. Joshi, E. Hedrick, S. Kumar, A. Yang, A. C. Pakpour-Tabrizi, A. Jindal, R. D. Chang, G. Cheng, N. Yao, R. J. Cava, N. P. de Leon, and A. A. Houck, Millisecond lifetimes and coherence times in 2D transmon qubits, *Nature*, 1 (2025).
- [48] D. Colao Zanuz, Q. Ficheux, L. Michaud, A. Orekhov, K. Hanke, A. Flasby, M. Bahrami Panah, G. J. Norris, M. Kerschbaum, A. Remm, F. Swiadek, C. Hellings, S. Lazăr, C. Scarato, N. Lacroix, S. Krinner, C. Eichler, A. Wallraff, and J.-C. Besse, Mitigating losses of superconducting qubits strongly coupled to defect modes, *Physical Review Applied* **23**, 044054 (2025).
- [49] M. Hegedüs, R. Banerjee, A. Hutcheson, T. Barker, S. Mahashabde, A. V. Danilov, S. E. Kubatkin, V. Antonov, and S. E. de Graaf, In situ scanning gate imaging of individual quantum two-level system defects in live superconducting circuits, *Science Advances* **11**, eadt8586 (2025).
- [50] Y. Kim, L. C. G. Govia, A. Dane, E. van den Berg, D. M. Zajac, B. Mitchell, Y. Liu, K. Balakrishnan, G. Keefe, A. Stabile, E. Pritchett, J. Stehlik, and A. Kandala, Error mitigation with stabilized noise in superconducting quantum processors, *Nature Communications* **16**, 8439 (2025).
- [51] D. S. Lvov, S. A. Lemziakov, E. Ankerhold, J. T. Peltonen, and J. P. Pekola, Thermometry based on a superconducting qubit, *Physical Review Applied* **23**, 054079 (2025).
- [52] M. Tuokkola, Y. Sunada, H. Kivijärvi, J. Albanese, L. Grönberg, J.-P. Kaikkonen, V. Vesterinen, J. Govenius, and M. Möttönen, Methods to achieve near-millisecond energy relaxation and dephasing times for a superconducting transmon qubit, *Nature Communications* **16**, 5421 (2025).
- [53] D. Wang, Y. Wu, N. Pieczulewski, P. Garg, M. C. C. Pace, C. G. L. Böttcher, B. Mazumder, D. A. Muller, and H. X. Tang, All-nitride superconducting qubits based on atomic layer deposition (2025), arXiv:2511.08931 [quant-ph].
- [54] S. Weeden, D. C. Harrison, S. Patel, M. Snyder, E. J. Blackwell, G. Spahn, S. Abdullah, Y. Takeda, B. L. T. Plourde, J. M. Martinis, and R. McDermott, Statistics of Strongly Coupled Defects in Superconducting Qubits (2025), arXiv:2506.00193 [quant-ph].
- [55] L. Chen, K.-H. Lee, C.-H. Liu, B. Marinelli, R. K. Naik, Z. Kang, N. Goss, H. Kim, D. I. Santiago, and I. Siddiqi, Scalable and Site-Specific Frequency Tuning of Two-Level System Defects in Superconducting Qubit Arrays (2025), arXiv:2503.04702 [quant-ph].
- [56] W. A. Phillips, Tunneling states in amorphous solids, *Journal of Low Temperature Physics* **7**, 351 (1972).
- [57] W. A. Phillips, Two-level states in glasses, *Reports on Progress in Physics* **50**, 1657 (1987).
- [58] C. Müller, J. H. Cole, and J. Lisenfeld, Towards understanding two-level-systems in amorphous solids: insights from quantum circuits, *Reports on Progress in Physics* **82**, 124501 (2019).
- [59] O. Oreshkov and T. A. Brun, Continuous quantum error correction for non-Markovian decoherence, *Physical Review A* **76**, 022318 (2007).
- [60] X.-Y. Guo, Thermalization and irreversibility of an isolated quantum system (2025), arXiv:2503.04152 [quant-ph].
- [61] X.-Y. Guo, Thermalization and irreversibility of an isolated quantum system II (2025), arXiv:2506.01351 [quant-ph].
- [62] J. Etxezarreta Martinez, P. Fuentes, P. Crespo, and J. Garcia-Frias, Time-varying quantum channel models for superconducting qubits, *npj Quantum Information* **7**, 115 (2021).
- [63] A. d. iOlius, J. E. Martinez, P. Fuentes, P. M. Crespo, and J. Garcia-Frias, Performance of surface codes in realistic quantum hardware, *Physical Review A* **106**, 062428 (2022).
- [64] J. Etxezarreta Martinez, P. Fuentes, A. deMarti iOlius, J. Garcia-Frias, J. R. Fonollosa, and P. M. Crespo, Multiqubit time-varying quantum channels for NISQ-era superconducting quantum processors, *Physical Review Research* **5**, 033055 (2023).